Fermilab

TM-1320
0451.000

ABORT KICKER POWER SUPPLY SYSTEMS AT FERMILAB*

G. Krafczyk, G. Dugan, M. Harrison, K. Koepke, and E. Tilles

June 1985

*Submitted to the 1985 Particle Accelerator Conference (NPS), Vancouver, British Columbia, Canada, May 13-16, 1985.

ABORT KICKER POWER SUPPLY SYSTEMS AT FERMILAB

G. Krafczyk, G. Dugan, M. Harrison, K. Koepke, E. Tilles
*Fermi National Accelerator Laboratory.
P.O. Box 500
Batavia, Illinois 60510

INTRODUCTION

Over the past several years, Fermilab has been operating with a single turn proton abort system in both the superconducting Tevatron and the conventional Main Ring[1,2]. The abort kicker power supply for this system discharges a lumped capacitance into the inductive magnet load, causing the beam to enter the abort channel. The characteristics of this current waveform are defined by the requirements of the machine operation. The standard fixed target running mode calls for 12 booster batches of beam which leaves a rotating gap in the beam of ~1.8 μs. The current waveform is required to rise to 90% of I_{max} in this time to avoid beam loss from partially deflected beam. Aperture limitations in both the accelerator and the abort channel demand that the current in the magnets stays above this 90% I_{max} for the 21 μs needed to ensure all the beam has left the machine. The 25 mm displacement needed to cleanly enter the abort channel at 1 TeV corresponds to a maximum current in each of the 4 modules of ~20 kA. Similar constraints are needed for the Main Ring and Tevatron antiproton abort systems.

A unique feature of this design is the high voltage, high current diode assembly used to clip the recharge of the capacitor bank. This allows the current to decay slowly with the L/R time constant of the magnet and diode series combination. Special attention will be given to the diode characteristics needed for this passive switching element. Operational experience and proposed upgrades will be given for the two operational systems.

CIRCUIT OPERATION

The pulsed power portion of the kicker is shown in Figure 1. Capacitor C is charged to an initial voltage V_c which is proportional to the energy of the beam. When an abort is called for, the thyratron switch (SW) is closed, pulling the positive end of C to ground. This reverse biases the diode string D and puts a negative voltage across the magnet L_{mag}. The components C_p and R_p are used to dampen high frequency reflections in the transmission line to the tunnel.

After SW is closed, the current in the magnet rises in an underdamped series resonant circuit composed of C, $L_T(L_{mag} + L_{cable})$ and ESR (equivalent series resistance). The ESR is composed of the tube drop, cable and magnet resistance, ESR of the capacitor, the reversed biased diode and the snubber network. The current versus time is given by

$$I_{mag} = \frac{V_c}{\left(\frac{L_T}{C} - \frac{ESR^2}{4}\right)^{1/2}} e^{-\frac{ESR}{L_T}t} \sin\left(\frac{1}{L_T C} - \frac{ESR^2}{4L_T^2}\right)^{1/2} t.$$

$$t_{peak} = \left(\frac{\frac{\Pi}{2}}{\frac{1}{L_T C}}\right)^{1/2} \quad \text{for} \quad \frac{ESR^2}{4L_T^2} << \frac{1}{L_T C}$$

At t_{peak}, the diode stack becomes forward biased and the current in it begins to rise. If the diode were considered perfect, the current would rise instantaneously and the voltage on the capacitor would remain at zero. This does not happen. During the time that the diode current is rising, voltage is building up on the capacitor in the reverse direction. This takes between 0.6 and 0.7 μs at which time the capacitor current reverses and further increases the current in the diode stack. The current in the capacitor relaxes again with the characteristics of an underdamped series RLC circuit which now is quite different since a very low resistance diode now shunts virtually all the current around the magnet inductance. Meanwhile, current slowly decays away with

$$\frac{di(t)}{i(t)} = \left(\frac{v_{diode}(i,t)}{i(t)\, L_T} + \frac{R_s}{L_T}\right) dt.$$

Operationally, The current is monitored in the cathode of the switch (CX1175B), and in the output transmission line (6-RG220's). As can be seen from Figure 1,

$$I_{mag} = I_{sw} + I_{diode}.$$

Representative current waveshapes for a Tevatron pulser are given in Figure 2. The current, I_{diode}, is obtained from the subtraction of the measured quantities I_{mag} and I_{sw}.

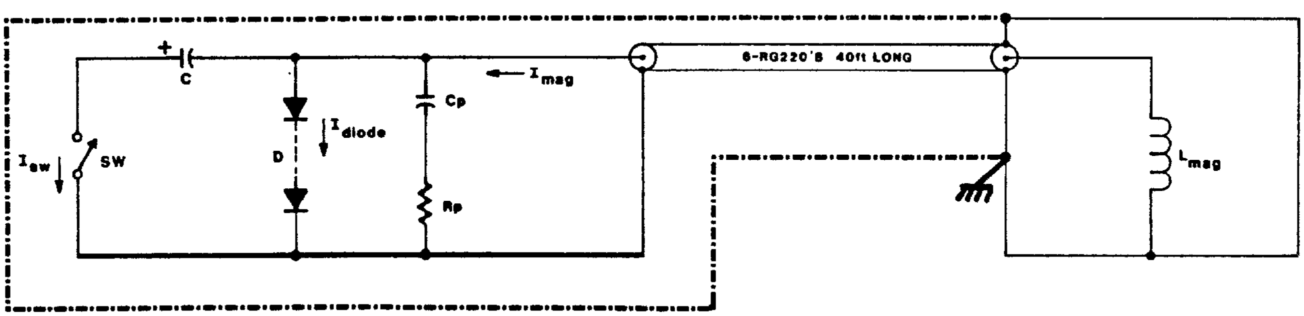

Figure 1. Simplified Pulse Power Circuit of Abort Pulser

*Operated by Universities Research Assoc., Inc. under contract to the U.S. Department of Energy

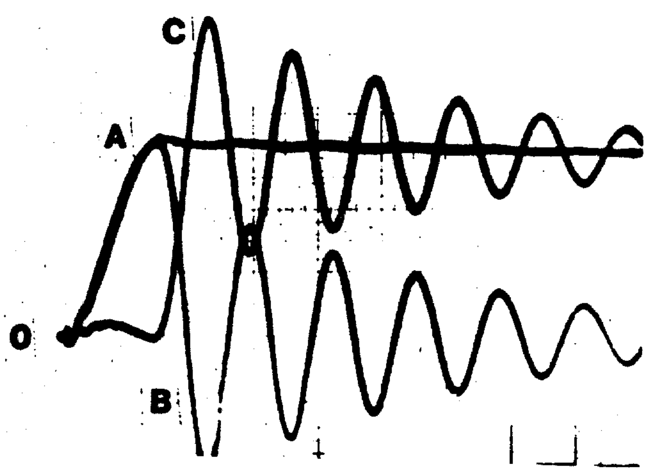

Figure 2. A) Magnet Current, B) Switch Current, C) Diode Current, V_c = 35 kV, All 5 kA/div, 2 μs/div

Each kicker system, even though operationally the same, has different parameters that relate to the particular application. These parameters are give in Table 1.

Table 1 Pulser Design Parameters

System	C	L_T	$(L_T/C)^{1/2}$	I_{mag}	# of Pulsers
MR p	.36uF	6.uH	4.1 Ω	8.2kA	2
TEV p	.72uF	4.uH	2.4 Ω	19.kA	4
TEV $\bar{p}$	.54uF	7.uH	3.6 Ω	10.5kA	3

DIODE SELECTION

The characteristics of the diode determines the shape of the kicker magnet current. The diode has to rapidly conduct at the peak of the current cycle. Otherwise, current will continue to decrease sinusoidally. This requires a large forward bias which can only come from rapid current decay in the kicker magnet. As soon as the diode is conducting, a minimum forward bias requirement for the diode reduces the rate at which current continues to decay in the magnet.

With this in mind, the following criteria for diode selection and construction were set:

(a) ~30% of the total kicker current variation during the 21 μs abort time (Δi/i) could come from the rise time of the current in the diode.
(b) ~40% of the total Δi/i could come from the dynamic forward resistance of the diode.
(c) ~30% of the total Δi/i could come from the series resistance of the magnet and cables.

In order to meet criteria (a), it is evident that a minimum inductance structure for the switch, capacitor, and diode are important. The physical dimensions of the whole structure were chosen to minimize this inductance. In the case of the diode, the inductance was minimized by stacking the diodes within a copper pipe to obtain a coaxial configuration. As tests proceeded, the largest contribution to this non-transfer of current from capacitor to diode came from the large diode dynamic impedance.

In order to choose a diode that satisfies criteria (a) and (b), a test circuit was constructed to drive a current through sample diodes and plot the voltage across the devices as a function of time. The circuit approximated a current source with a rise time of about 200 ns. No data was taken for the first 400 ns to allow time for the Ldi/dt effects of the test circuit to disappear.

From a scope trace of diode voltage versus time at a constant current, the integral of the diode impedance for the time interval of .4 to 21 μs was obtained. The total dynamic resistance is proportional to the number of series diodes required to withstand the total capacitor voltage.

Figure 3 is a representative picture of the voltage across several diodes versus time. The higher voltage device (R720-4406) has a much higher initial voltage and takes a longer time to decay. This in itself is not necessarily bad since you will need fewer of these higher voltage devices to produce a diode with a V_{RRM} of 50 kV.

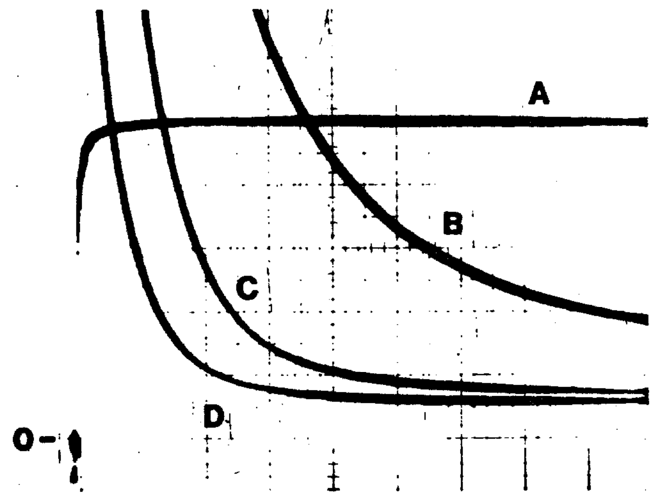

Figure 3. A) Test current, 200 A/div, B-D) Diode forward voltage, 2 V/div, B) R720-4406, C) R 920-1816, D) 2001-PDK-160, All 1 μs/div

Table 2 gives parameters for various diodes measured. Higher current devices are preferred since with the high peak currents, reliability is always a problem.

Table 2 Measured Diode Parameters

Diode Type	V_{RRM} (V)	I_F(avg) (A)	Figure of Merit*
R920-1816	1000	1800	1.7
R9G0-1222	2200	2200	1.8
R9G0-1622	1600	2200	1.4
R9G0-4212	4200	1200	2.2
R720-4406	4400	600	2.1
2001-PDK-160	1600	2000	.95
1601-PDK-250	2500	1600	.83
851-PDE-160	1600	850	.78

$$* \text{ Figure of Merit} = \frac{50 \text{ kV}}{V_{RRM} \times 1 \text{ kA}} \int_{.4\ \mu s}^{21\ \mu s} v_{diode}(t)\ dt$$

The device that was chosen is the International Rectifier 2001-PDK-160. Tests showed that V_{RRM} for typical devices was about 1.9 kV. Thus, fewer devices in the stack were needed.

Criterion (c) was reasonably straight forward to meet. The magnet conductors were chosen with surfaces that have a minimum radius if 0.25 in, with total circumference of about 6 in (high voltage requirement). This gives a skin depth dominated resistance of $\sim 2 \times 10^{-3}\,\Omega$ at 100 kHz. The dc value of the magnet resistance is $\sim 0.13 \times 1^{-3}\,\Omega$.

The transmission line is composed of 6 - RG220's, about 40 feet long, giving a 100 kHz resistance of $\sim 8 \times 10^{-3}\,\Omega$ and a dc resistance of $\sim 1 \times 10^{-3}\,\Omega$.

The frequency of interest can be approximated by a sine wave with a period of ~40 us which corresponds to a frequency of ~25 kHz. This brings the aver--- resistance of the magnet and transmission line t $\sim 5 \times 10^{-3}\,\Omega$ or less, giving a decay well within criteria (c).

OPERATIONAL EXPERIENCE

Two Main Ring and four Tevatron pulsers have been operating for about two years. The Main Ring pulsers have $\sim 10^{6}$ pulses and the Tevatron pulsers have $\sim 2 \times 10^{5}$ pulses on them. The most obvious and disconcerting problem that has occurred is catastrophic magnet failures. In all cases to date, the failures have occurred within the magnet at a highly stressed place. When the magnets are taken apart, there are a number of bubbles in the insulation (Dow Corning Sylgard #184). Since the nominal stress is well below the breakdown of the rubber, it is felt that the problem originates from a bubble which ionizes and eventually spreads to create final failure.

A representative picture of the current in a magnet that has failed is given in Figure 4. This particular magnet is from our Main Ring system that failed recently. Trace A is a nominal magnet current pulse at V_c = 8kV (voltage lower than breakdown) and trace B is magnet current pulse at V_c = 13kV (voltage greater than breakdown). The initial current rises much faster (lower L) at first but the current is traveling through an arc. Thus the faster decay after the current peak. As the current fills the whole magnet and extinguishes the arc, the current decays normally (di/dt similar to trace A).

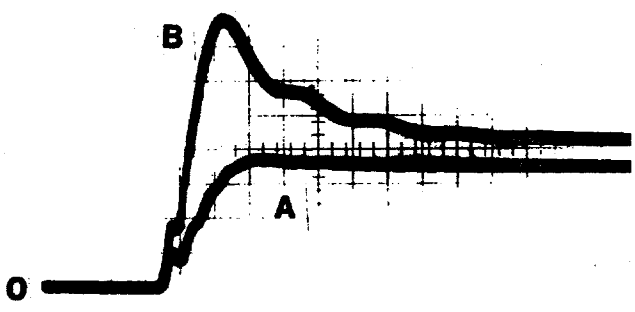

Figure 4. A) Normal magnet current, V_c =8 kV,
B) Magnet current under fault condition,
V_c =13 kV, 2 kA/div, 2μs/div

The second most troublesome failure is with the energy storage capacitors. As failures occur, they are being replaced by higher current, 90% reversal, higher voltage units specified with actual current wave shapes.

Almost no problems have been observed with the hydrogen thyratrons used as the main switch (English Electric Valve CX1175B). A few prefires have been observed, but to date, all have been attributed to partial discharge of the energy storage capacitors creating noise which triggers the tube. This problem has been non-existent during the first 5 months of the 1984-1985 run.

The diodes (thought to be the most technically difficult) have been the most trouble free device of the system. Even with the magnet failures, forcing as much as twice the design current through the devices, no failures to date have occurred.

PROPOSED UPGRADES

The most significant improvement to the system and one that will be implemented in the Tevatron antiproton systems, will be the addition of a small (0.1-0.2Ω) resistance in series with the capacitor and switch. This resistance will increase the damping which will improve the capacitor and switch life. The system must now operate at a higher initial voltage. For the Tevatron antiproton and the Main Ring proton systems, this should not be a problem. For the Tevatron proton systems, this higher voltage may not be possible.

Another proposed improvement would be to move the snubber network (R_p and C_p) from the transmission line input to the magnet input. In the Tevatron antiproton systems, we expect to increase the impedance of the transmission line to 25Ω after which C_p should not be needed. If this is successful, the Main Ring proton systems may also be modified.

At present, the magnet current shapes are displayed in the control room via a TV monitor. An improvement would be to digitize the signal and insert it into the control system. This type of monitor would allow precise timing measurements and simplify alarm and limit controls.

ACKNOWLEDGEMENTS

We thank the Accelerator Mechanical Kicker Group for their work to build the original MR and TeV proton systems and their continued support at building the TeV antiproton systems. Thanks is also given to Mark Mills and Mark Lamers for their help in maintaining the abort kicker systems.

REFERENCES

1. Design Report, 1979 Superconducting Accelerator, Fermilab (1979).

2. G. Krafczyk, et.al., "A 3 kG Kicker Magnet System for the Tevatron Beam Abort System," IEEE Trans. NS-28, June 1981.